STUDY OF THE EVOLUTION OF THE Cu/Nb INTERPHASE BOUNDARY BY THE MOLECULAR DYNAMICS METHOD

I. V. Nelasov, A. G. Lipnitskii, and Yu. R. Kolobov   UDC 537.9: 539.213

The evolution of atomic structure of the interphase boundary for composites from immiscible Cu/Nb elements is studied by the molecular dynamics method. It is established that the planar interphase boundary is stable at temperatures up to 1200 K. Atomic dissolution of elements is not revealed in the entire examined temperature interval, and the components are mixed on the interphase boundary of finite curvature in the form of clusters and nanolamellas; moreover, the amorphous state is not formed in the process of migration of the interphase boundary.

Keywords: metal composites, interphase boundary, amorphization, copper–niobium.

INTRODUCTION

The materials comprising nanodimensional microstructures have attracted scientific and practical interest due to their extraordinary properties. Special attention is given to nanocomposites of immiscible metals (Cu–Nb, Cu–Ta, etc.). Materials of this group, being widely used superconductors, are simultaneously resistant to radiative damage [1, 2]. The interphase boundary plays an important role in the process of annihilation of radiative defects and suppression of blister growth in Cu/Nb systems with layer thickness of about 2.5 nm [1]. Therefore, of scientific and technological interest are the stability of the interphase boundary and the mechanisms of evolution of its atomic structure.

The data on amorphization of the interphase boundary of immiscible elements available from the literature are contradictory. On the one hand, the absence of amorphization on the Cu/Nb interphase boundary irradiated by He ions with energies of 33 and 150 keV and subsequent annealing at 873 K was noted in [1]. In addition, the temperature stability of this system during vacuum annealing at a temperature of 1073 K was also indicated in [1]. According to [3], the interface of the (Co: 5 nm/Cu: 5 nm) system remained stable during annealing at 923 K for 4 h. In [4] it was established that in the process of amorphization during which unstable β-Ta was formed on the interphase boundary of the Cu–Ta laminate prepared by deposition, the amorphous zone was formed on the interphase boundary only during β-Ta → α-Ta phase transition; it vanished after the termination of the phase transformation during annealing at 1073 K, whereas the α-Ta–Cu interphase boundary remained stable at this temperature.

On the other hand, the occurrence of amorphous zones on the boundary in the Cu–Nb system was pointed out in [5, 6]. In these works, the formation of the amorphous phase was explained by the process of relaxation of mechanical stresses accumulated on the interphase boundary in the process of composite manufacturing. It should be noted that changes of the interphase boundary or particles and hence migration of the interphase boundary accompanying these changes were also pointed out in [4–6] where the amorphization was established.

The molecular-dynamics modeling allows detailed information on the processes in nanostructural materials to be obtained. This method was used to investigate the mechanism of forming the amorphous layer in composites of immiscible components and the proportion of elements at which the amorphous phase was formed when atoms in the matrix of the first metal were randomly replaced by the second metal and subsequently annealed on the example of Sc–W [7] and Cu–Ta systems [8]. Results of modeling demonstrated that when the initial material had a layered structure, the amorphization was not observed for systems with positive enthalpy of Co–Cu and Cu–Nb mixtures [9]. Results of

TABLE 1. Calculated Characteristics of the Niobium BCC Lattice in Comparison with the Available Experimental Data and Results of *ab initio* Calculations. Here a_0 Is the Lattice Constant; Ω Is the Atomic Volume; E_{sub} Is the Sublimation Energy; B and B' Are the Bulk Modulus and Its Derivative with Respect to Volume; C_{11}, C_{12}, and C_{44} Are the Elasticity Moduli; E_V^f and E_V^m Are Energies of Vacancy Formation and Migration; Ω_V^f Is the Volume of Vacancy Formation in Fractions of the Atomic Volume Ω; Q_m is the Self-Diffusion Activation Energy; γ Is the Surface Energy; and $\Delta E_{BCC\text{-}FCC}$ is the Energy Difference for the FCC and BCC Lattices

Characteristics	Our EAM	Experiment or *ab initio* calculations	Characteristics	Our EAM	Experiment or *ab initio* calculations
a_0, Å	3.30	3.30	E_V^m, eV	0.66	0.55
Ω, Å^3	18.0	18.0	Q_m, eV	3.39	3.6
E_{sub}, eV	7.57	7.57	$\gamma(110)$, J/m^2	2.32	1.79–2.9
B, GPa	170	170			
B'	4.1	4.1	$\gamma(100)$, J/m^2	2.44	2.7
C_{11}, GPa	241.9	245			
C_{12}, GPa	133.5	133.2	$\gamma(111)$, J/m^2	2.82	2.7
C_{44}, GPa	27.8	28.4			
E_V^f, eV	2.73	2.75	$\Delta E_{BCC\text{-}FCC}$, eV/atom	0.37	0.22
Ω_V^f, Ω	0.39	0.45			

TABLE 2. Energy E_F of the Cu–Nb Model System Formation Calculated with the EAM Potentials in Comparison with the Results of *ab initio* Calculations

Characteristic		Cu$_3$Nb	CuNb	Nb$_3$Cu	Nb$_9$/Cu$_{12}$
E_F, eV/atom	EAM	0.31	0.19	0.13	0.15
	ab initio	0.35	0.20	0.13	0.12

modeling presented in [9] together with investigations by the methods of transmission electron microscopy and Auger electron spectroscopy [10] demonstrated that primarily amorphous interphase boundary was stratified in the process of laminate manufacturing, which is explained by the positive enthalpy of mixing.

The present work is aimed at testing the assumption that the amorphization of the interphase boundary in the Cu–Nb system is caused by migration of the boundary and at investigating the evolution of the atomic structure in this process.

METHOD AND RESULTS OF MODELING

In the molecular-dynamics modeling by the embedded-atom method (EAM), the well-approved copper potentials constructed by Mishin [11] were used. The EAM potentials for niobium and the pairwise copper–niobium potentials were constructed based on the experimental data and results of *ab initio* calculations using the software package *ABINIT* [12]. Table 1 presents the niobium characteristics calculated with the given potentials in comparison with the experimental data and results of our *ab initio* calculations. Table 2 gives the results of our calculations of the energy characteristics of the model copper–niobium systems in various configurations.

To study the process of amorphization of the interphase boundary during its migration in the Cu–Nb system, the initial stage of niobium disk evolution in the copper matrix was modeled on a computer (Fig. 1). A 245 × 212 × 56 Å copper sample comprising the niobium disk with a radius of 50 Å, thickness of 20 Å, and a curvature radius of the disk edge of 10 Å was modeled. The periodic boundary conditions were used. When the Nb disk was incorporated into the copper volume, the same copper disk was extracted from it. The (111) copper plane
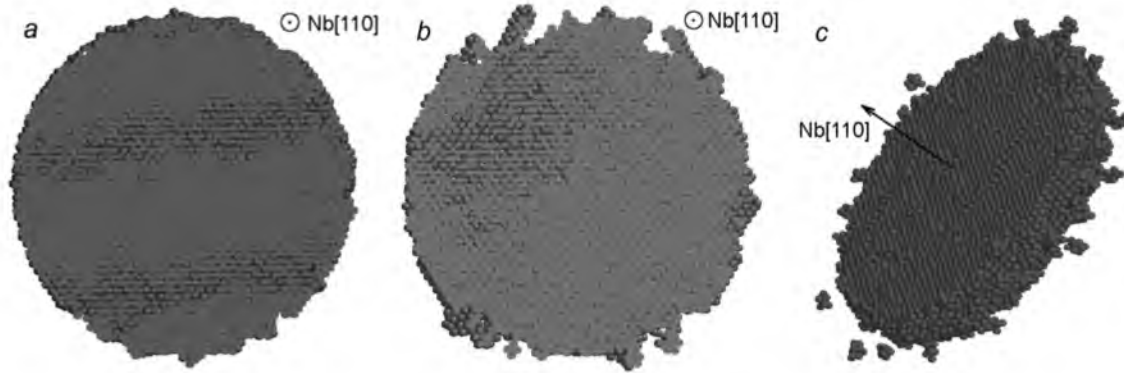
Fig. 1. Cuts of the niobium disk after annealing *a*) at 900 K for 20 ns and *b*) at 1200 K for 30 ns; *c*) the niobium disk in melted copper after annealing at 1500 K for 0.5 ns. Only Nb atoms are shown.

bordered with the (110) niobium plane. The initial minimal distance d_{min} between the niobium and copper atoms was chosen for thermodynamic pressure minimization. After that, the system relaxed to a pressure of $1 \cdot 10^{-3}$ GPa and to maximum forces acting on each atom no more than 5 meV/ Å .

Analogously, the sample of nanostructural composite with layered structure comprising niobium and copper layers with thickness of 4.6 nm was modeled. To provide periodic boundary conditions for the arrangement of the (111) copper surface on the (110) niobium surface, the Nishiyama–Wasserman orientation was used.

The model samples with disk-shaped copper inclusions were subjected to heating and molecular-dynamics annealing to temperatures of 300 and 600 K for 7 ns for samples at 300 and 600 K and for more than 20 ns for samples at 900 and 1200 K. The system state was registered every 1 and 0.5 ns, respectively. In addition, the samples were subjected to heating and annealing at 1500 K for 0.5 ns, at 1800 K (above the temperature of copper melting) for 0.25 ns, and at 3500 K (above the temperature of niobium melting) for 1 ns. The Cu/Nb model nanolaminate sample was subjected to annealing at 900 and 1200 K for 20 ns.

The results of modeling demonstrated that the interphase boundary at temperatures below 900 K remained unchanged. As can be seen from Fig. 1*a*, niobium nanolamellas are formed at 900 K. Figure 1*b* illustrates the evolution of this process at 1200 K. At temperatures of copper melting and higher (Fig. 1*c*), the nanolamellas are separated, and niobium clusters with sizes of (5 ± 0.8) Å comprising 7–12 niobium atoms are formed in copper. Thus the stationary planar interphase boundary remains stable (for temperatures below that of copper melting and indicated time periods) for the composite with niobium disk inclusion and nanolaminate.

For all temperatures, the incorporation of niobium into copper atoms and copper into niobium atoms was not observed in the model, including temperatures exceeding melting ones for the components of the composite. This suggests possible niobium mass transfer through the copper volume by the mechanism of cluster migration rather than by diffusion of individual niobium atoms.

The dependences of the increase in the relative number of atoms of one element surrounded by another element in the composite (Fig. 2) confirm the high stability of the planar copper–niobium interphase boundary. After cooling of the examined model samples, local distortions of the copper lattice were observed in the vicinity of nanolamellas and niobium clusters. This can explain regions of broadening and amorphization observed on the interphase boundary as a result of spheroidizing of niobium inclusions observed in [6] by the method of high-resolution electron microscopy by distortion of the lattices other than by actual amorphization on the atomic level.

The radial distribution functions (RDFs) of atoms on the interphase boundary of the disk were obtained. The RDF was constructed for two samples after molecular-dynamics annealing, namely, for the reference sample (annealed at 300 K for 7 ns) and for the sample (annealed at 1200 K for 30 ns) cooled to 300 K for rightfull comparison with the reference sample. To draw the RDF, the density of atoms in the spherical layer ρ was normalized to the average density of copper and niobium atoms ρ_0. Figure 3 shows the Cu–Cu and Nb–Nb RDFs of the above-indicated systems.
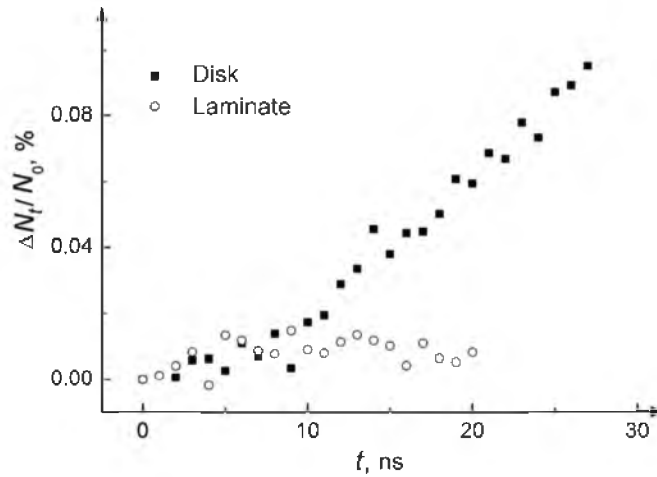
Fig. 2. Changes in the number of atoms on the interphase boundary ΔN_t with time t normalized to the initial number of atoms N_0 during annealing of composites with the indicated structures at 1200 K.
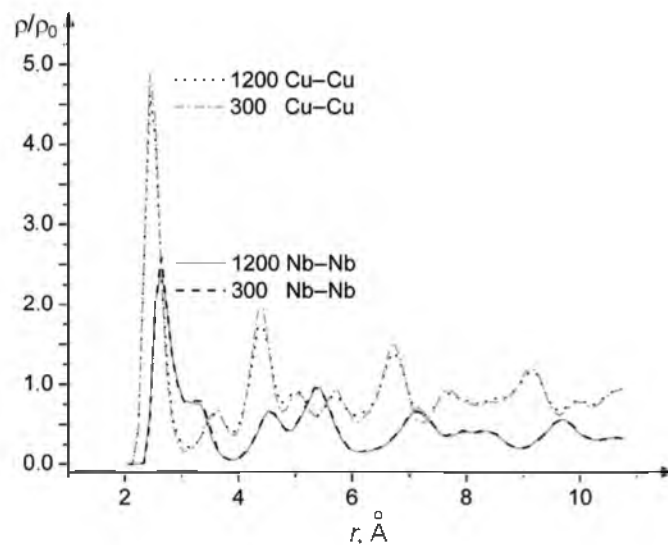

Fig. 3. Radial distribution functions of atoms on the copper–niobium boundary.

Changes of the RDF peaks on the examined Cu/Nb interphase boundary in comparison with the RDFs of ideal FCC and BCC states is mainly caused by the system geometry, since the atom of one species is surrounded by atoms of another species. Smearing of the coordination spheres near the interphase boundary, caused by local distortions of the atomic structure, is also observed. A decrease in the RDF peak amplitudes for the sample annealed at 1200 K compared to the reference sample corresponds to the change of the partial structure of neighboring atoms for niobium in calculation of the radial distribution function. For example, a decrease of the first Nb peak amplitude after annealing by 1.6% corresponds to an increase in the relative fraction of the Cu atoms in the local Nb surrounding also by 1.6%. A decrease of the peak amplitudes in copper after annealing can be attributed to an increase in the partial fraction of Nb atoms only partly. It seems likely that it is caused to a greater degree by redistribution of copper atoms accompanying changes of the local surrounding.

TABLE 3. Distances for the Coordination Spheres on the Interphase Boundary and in the Volume of the Material, Å

Structures	$r1$	$r2$	$r3$	$r4$
Cu FCC	2.55	3.615	4.43	5.10
Nb BCC	2.85	3.30	4.67	5.48
Nb on the interface boundary	2.67	3.28	4.59	5.45
Cu on the interface boundary	2.51	3.62	4.43	5.10

TABLE 4. Ratios of the Radii of the 2nd–4th Coordination Spheres to the Radius of the First Coordination Sphere Based on the Results of Our Calculations in Comparison with the Experimental Data and Amorphous Structure Models [13, 14]

Structures	$r2/r1$	$r3/r1$	$r4/r1$
Nb BCC	1.15	1.63	1.91
Nb on the interface boundary	1.23	1.72	2.04
Cu FCC	1.41	1.73	2.00
Cu on the interface boundary	1.44	1.76	2.03
Experimental data [13, 14]			
Amorphous iron film	1.67	1.96	2.51
Liquid iron	1.85	–	2.73
Liquid copper	1.87	–	–
Liquid copper (*ab initio*)	1.83	–	–
Amorphous structure models [13]			
Finney	1.73	2.00	2.65
Sadoka	1.66	2.00	2.60
Yamamoto	1.66	1.97	2.48

From Fig. 3 it can be seen that the position of peaks in the RDF remains stable, because the RDF values in the initial state and after molecular-dynamics annealing virtually coincide for each element. An analysis of peak positions demonstrates that the maximum of the first coordination sphere on the niobium interphase boundary is at 2.7 Å, whereas in the niobium single crystal and in the middle of the disk, the maximum is at 2.85 Å. The same is true for the distance to the first copper coordination sphere: it is 2.45 Å on the interphase boundary and 2.55 Å in the ideal FCC and in copper volume far from the interphase boundary. These changes are most likely due to reorganization of atoms near the interphase boundary. Positions of the second, third, and fourth coordination spheres do not differ from those for the ideal lattice.

The radii of coordination spheres on the interphase boundary in comparison with those for pure copper and niobium at 300 K are given in Table 3. According to the amorphization criteria [13], the examined Cu/Nb interphase boundary is not amorphous. This is indicated by 1) the absence of peak splitting for the second coordination sphere in the plots of Cu–Cu and Nb–Nb RDFs, and 2) the fact that the ratio of radii of the second, third, and fourth peak to the radius of the first peak does not correspond to the amorphous state. These ratios of the peak radii in comparison with the corresponding ratios for the amorphous structures and ideal FCC and BCC lattices are given in Table 4. An insignificant increase in the ratios of peak radii on the interphase boundary is due to a decrease in the distance at which the first peak is observed. With increasing distance from the boundary, its influence also weakens, and the ratios of the third and fourth peak radii to the second peak radius remain unchanged and typical for the ideal crystal state. Therefore, from the results of comparison of the peak radius ratios for the experimental data and the results of modeling we can conclude that the amorphous state is absent on the interphase boundary in the process of modeling of its evolution.

Our investigations allow us to conclude that amorphization on the copper–niobium interphase boundary is absent. The structures observed on the interphase boundary in [5, 6] and identified by the methods of transmission

electron microscopy as amorphous ones arose due to migration of the interphase boundary caused by stresses accumulated in the process of material manufacturing. In this case, niobium was dissolved in the copper matrix in the form of nanoclusters. These processes were not observed in the nanolaminates manufactured by deposition, and the structure of their interphase boundary remained stable [1–4]. This conclusion has also been confirmed recently in [15] in which the film manufactured by simultaneous copper and niobium deposition was studied by the methods of transmission microscopy and three-dimensional atom probe tomography. Results of investigations demonstrated stratification of elements in the deposition stage, which was intensified during annealing at 473 K for 11 h and caused further stratification of copper and niobium with the formation of nanodimensional regions with sizes of 2–3 nm that differed by the elemental composition. Based on the data obtained, this can be explained by mutual dissolution of cluster elements.

CONCLUSIONS

The molecular-dynamics modeling of migration of the Cu/Nb interphase boundary has demonstrated incorporation of nanolamellas of one metal into another with subsequent formation of isolated monatomic clusters. The crystal structure was distorted in cluster and lamella regions, which could be perceived as amorphization of the interphase boundary in studies by the methods of high-resolution microscopy. The radial distribution function of atoms on the migrating Cu/Nb interphase boundary remained unchanged, which demonstrated the absence of boundary amorphization in this process.

REFERENCES

1. A. Misra, M. J. Demkowicz, X. Zang, and R. G. Hoagland, J. Miner. Met. Mater. Soc., **58**, No. 9, 62–65 (2007).
2. M. J. Demkowicz, R. G. Hoagland, and J. P. Hirth, Phys. Rev. Lett., No. 100, 136102(1)–136102(4) (2008).
3. A. Ullrich, M. Bobeth, and W. Pompe, Int. Sci., No. 12, 249–257 (2004).
4. H.-J. Lee, K.-W. Kwon, C. Changsub, and R. Sinclair, Acta Mater., **47**, No. 15, 3965–3975 (1999).
5. X. Sauvage, L. Renaud, B. Deconihout, et al., Acta Mater., No. 49, 389–394 (2001).
6. K. H. Lee and S. I. Hong, Mater. Sci. For., **503-504**, 907–912 (2006).
7. R. F. Zhang, Y. Kong, and B. X. Liu, Phys. Rev. **B**, No. 74, 214102(1)–214102(8) (2005).
8. H. R. Cong, L. T. Kong, W. S. Lai, and B. X. Liu, Phys. Rev. **B**, No. 66, 104204(1)–104204(9) (2002).
9. M. J. Demkowicz and R. G. Hoagland, J. Nucl. Mater., No. 372, 45–52 (2008).
10. J. Thomas, A. John, et al., Microchim. Acta, No. 133, 131–135 (2000).
11. Y. Mishin, M. J. Mehl, D. A. Papaconstantopoulos, et al., Phys. Rev., **B63**, 224106–224122 (2001).
12. X. Gonze, J.-M. Beuken, R. Caracas, et al., Comp. Mater. Sci., No. 25, 478–492 (2002).
13. K. Sudzuki, X. Fudzimori, and K. Xasimito, Amorphous Metals [Russian translation], Metallurgiya, Moscow (1987).
14. A. Pasquarello, K. Laasonen, R. Car, et al., Phys. Rev. Lett., **69**, No. 13, 1982–1985 (1992).
15. A. Puthucode, M. J. Kaufman, and R. Banerjee, Met. Mater. Trans., **A39**, 1578–1584 (2008).